Structural, electrical, and optical characterizations of epitaxial $Zn_{1-x}Ga_xO$ films grown on sapphire (0001) substrate

Michael Snure and Ashutosh Tiwari[a)]
Nanostructured Materials Research Laboratory, Department of Materials Science and Engineering, University of Utah, Salt Lake City, Utah 84112

(Received 13 March 2007; accepted 15 May 2007; published online 28 June 2007)

In this paper we report the structural, electrical, and optical properties of epitaxial $Zn_{1-x}Ga_xO$ films (x=0–0.05) grown on single crystal sapphire (0001) substrate by pulsed laser deposition technique. Structural and elemental analysis was performed using high-resolution x-ray diffraction (θ-2θ and Φ scan) and energy dispersive x-ray spectroscopy. Temperature dependent electrical resistivity and thermoelectric power measurements were performed over the temperature range of 77–300 K and 296–373 K, respectively. Hall effect and optical transmission measurements were preformed at room temperature. All these studies showed that the structural, electrical as well as the optical characteristics of $Zn_{1-x}Ga_xO$ films depend very sensitively on the Ga contents. As the Ga doping concentration is increased, initially an increase in carrier concentration and optical band gap is observed (until x=0.04), which is followed by a decrease at higher concentrations. These features were attributed to the combined effect of band filling (Burstein-Moss effect), electronic correlation, and epitaxial strain present in the system. Above parameters also affected the electrical properties of the films quite significantly. $Zn_{1-x}Ga_xO$ films with 1% of Ga doping (x=0.01) showed metal-like electrical resistivity. However, for higher doping levels, enhanced scattering potential, arising from randomly distributed impurity atoms, resulted in the Anderson localization of electronic states.
 [DOI: 10.1063/1.2749487]

INTRODUCTION

Transparent interconnects made using transparent conducting oxides (TCOs) are considered one of the most important components of light emitting diodes (LEDs), solar cells, flat panel displays, and other modern optoelectric devices.[1] Indium tin oxide (ITO) is currently the most widely used TCO for optoelectronic applications.[1,2] ITO has served as a workhorse for the TCO industry for quite a long time. But it is anticipated that a stable supply of ITO may be difficult to maintain for the recently expanding market of optoelectronic devices because of the scarcity of indium, the principal component of ITO. Moreover ITO suffers the disadvantages of poor chemical and thermal stability.[2] These factors have led researchers to search for alternate materials for TCO applications.

Some of the alternative TCO materials that have been studied for transparent electrode applications are (Ga, Al, In):ZnO, $(F,Sb):SnO_2$, and $Nb:TiO_2$.[3–6] Among these alternatives, ZnO of the II-IV semiconductor family stands out as the most promising candidate because of its low cost, relatively high abundance, and good optical and electrical properties. ZnO is an intrinsic n-type semiconductor with a large band gap (3.3 eV) and high exciton bonding energy (60 meV).[3,4] Nonstoichiometric ZnO has been extensively studied as a possible transparent conductor. ZnO films with a high density of oxygen vacancies have shown resistivities as low as 1×10^{-2} Ω cm and optical transmission of about 88% but are unstable at high temperature and in oxidizing environments.[7,8] Therefore, for more practical applications, ZnO films doped with group III elements (Al, Ga, or In) are being perused. Among these, Al doped ZnO has been the most widely studied system so far.[7] However, recently some very interesting and promising results have been reported for Ga doped ZnO films. Compared to Al, Ga is far less reactive and is more resistant to oxidation.[9,10] Also, the covalent bond length of Ga–O (1.92 Å) is very close to that of Zn–O (1.97 Å),[11] which may result in high electron mobility and low electrical resistivity for high Ga doping concentrations.

Motivated by the potential of Ga doped ZnO as a cost effective TCO material, here we report a systematic study of the effect of doping Ga on the structural, electrical, and optical properties of ZnO films. Epitaxial $Zn_{1-x}Ga_xO$ films were grown on sapphire (0001) substrates and the Ga doping concentration was systematically varied in the range of 0–5 at. %.

EXPERIENTIAL PROCEDURE

All the thin film samples investigated in this study were prepared by pulsed laser deposition (PLD) technique. High purity single-phase bulk targets used for laser ablation were prepared by sol-gel technique. Details about this technique have been published somewhere else.[12] Targets were transferred to a stainless steel vacuum chamber for laser ablation. A KrF pulsed excimer laser (248 nm wavelength and pulse width of 25 ns) was used for ablating the targets. The PLD chamber was pumped down to a base vacuum of 10^{-6} Torr. Then the films were deposited on sapphire (0001) substrate with an energy density of 2–4 J/cm^2 at a pulse repetition

a)Electronic mail: tiwari@eng.utah.edu

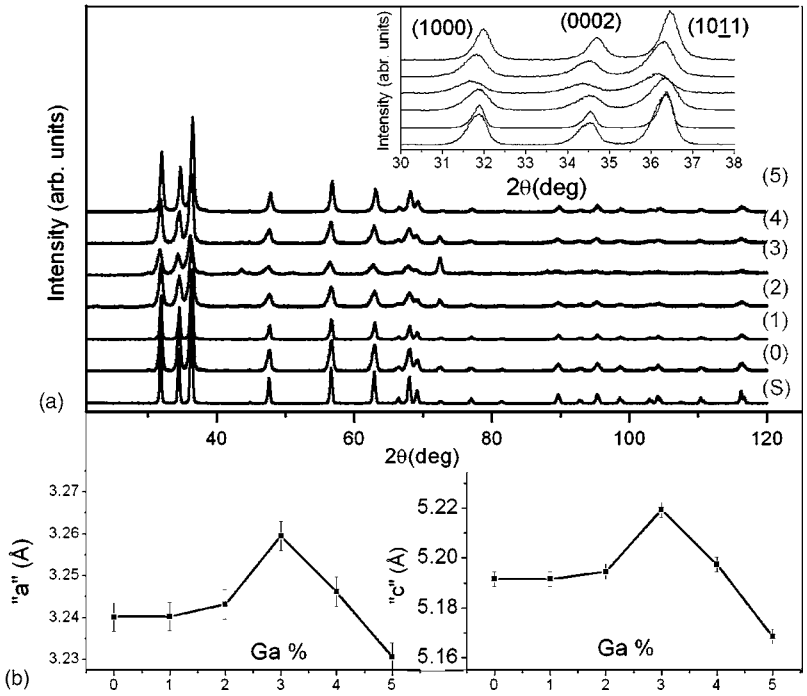

FIG. 1. (a) X-ray θ-2θ diffraction patterns of $Zn_{1-x}Ga_xO$ (x=0–0.5) powders. Inset is a close-up of the first three peaks, (1000), (0002), and (10$\bar{1}$1). Labels (0)–(5) correspond to at. % Ga concentration and (s) is undoped ZnO. (b) Variation of lattice parameters a and c with gallium doping concentration (x).

rate of 10 Hz and substrate temperature ~650 °C. The thickness of various films investigated in this work was about 200 nm.

Samples were characterized by x-ray diffraction (XRD), energy dispersive x-ray spectroscopy (EDS), and optical transmission spectroscopy. Both θ-2θ and Φ x-ray scans were preformed using Cu $K\alpha$ radiation with a Ni filter. Chemical composition was determined using an EDAX 3000-N detector. The optical transmission measurements were preformed using a DU 730 UV/visible scanning spectrophotometer in wavelength scanning mode. Electrical conductivity of the films was measured using a four-probe technique in the temperature range of 77–300 K. Thermoelectric power was measured over the temperature range of 296–373 K. For these measurements a temperature difference ΔT of 5 K was applied across the samples and the voltage difference ΔV, thus developed across the sample, was measured using copper thermocouple wires. The ratio $\Delta V/\Delta T$ gives the thermoelectric power of the sample with respect to copper. Absolute thermoelectric power was obtained by adding to this the absolute thermoelectric power of copper. Hall effect measurements were preformed at room temperature to obtain the concentration and mobility of charge carriers in the samples.

RESULTS AND DISCUSSION

Figure 1(a) shows the XRD patterns of $Zn_{1-x}Ga_xO$ (x =0–0.05) targets prepared using our previously developed sol-gel technique,[12] Diffraction patterns of all the samples match very well with that of ZnO reference pattern. No additional peaks could be identified in any of the samples implying they are single phase. However, there is a considerable amount of peak broadening and shifting as compared to the coarse ZnO precursor material. This can be seen in the inset of Fig. 1(a), which shows a close up of the first three peaks, (100), (002), and (101). The broadening of the peaks is caused by the reduction of crystallite size and peak shifting is caused by changes in the lattice spacing as Ga is substituted into the system. Figure 1(b) shows the variation of lattice parameters a and c for different samples as a function of Ga concentration. There is an increase in both a and c until a maximum is reached at 3% Ga doping. As Ga doping passes 3%, lattice spacing decreases. Though the final decrease in the lattice volume for higher Ga concentrations can be attributed to the smaller size of Ga ions compared to Zn, the initial increase in lattice volume for lower Ga concentrations is indeed quite intriguing. We believe that apart from the smaller size of Ga, the increased number of charge carriers introduced by Ga may also be playing an important role. Since the samples are nanocrystalline, carriers will be confined to nanosized grains producing a repulsion which can result in an expansion in the lattice volume.[13,14] More work is going on to understand the real mechanism responsible for the variation of lattice volume in nanocrystalline $Zn_{1-x}Ga_xO$. Those results will be published somewhere else. In the rest of this paper, our main focus will be on epitaxial thin film samples.

Figure 2(a) shows a typical θ-2θ x-ray diffraction pattern from $Zn_{1-x}Ga_xO$ films with x=0–0.05. Only the diffraction peaks corresponding to (000l) family of planes of wurtzite $Zn_{1-x}Ga_xO$ are observed indicating strong c-axis alignment of the film. No additional peaks were found indicating the absence of additional phases like Ga_2O_3 precipitates in the films. The θ-2θ scans give information about the out-of-plane orientation only, so in order to determine in-plane orientation of the films, azimuthal Φ-scans were performed. Figure 2(b) shows the four-circle high-resolution x-ray Φ scan from $Zn_{1-x}Ga_xO$ film for (10$\bar{1}$1) plane. The Φ-scan

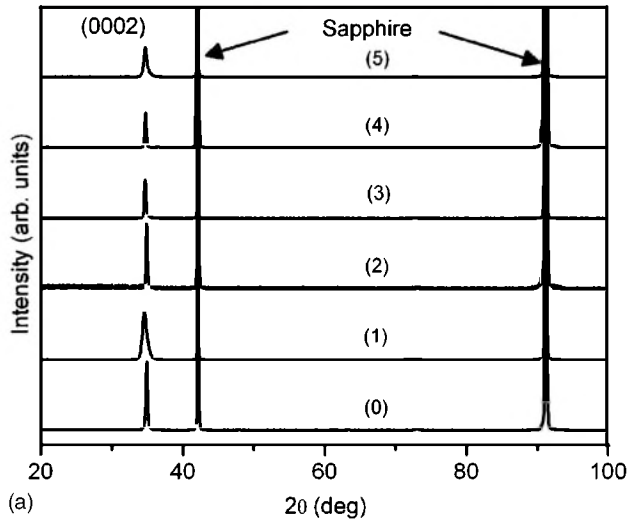

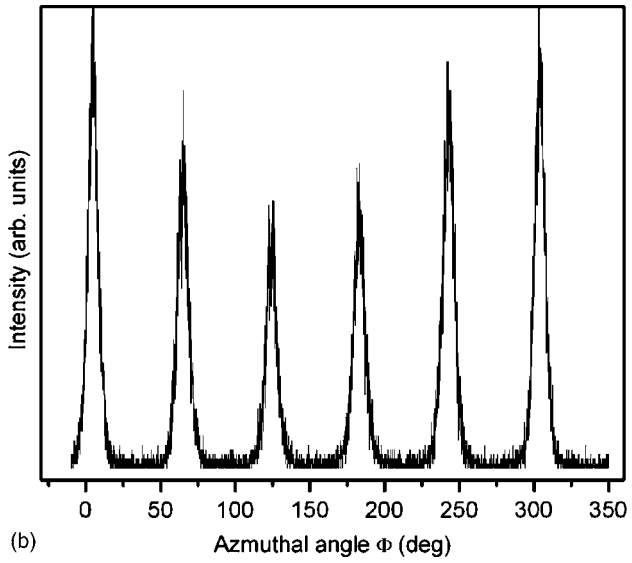

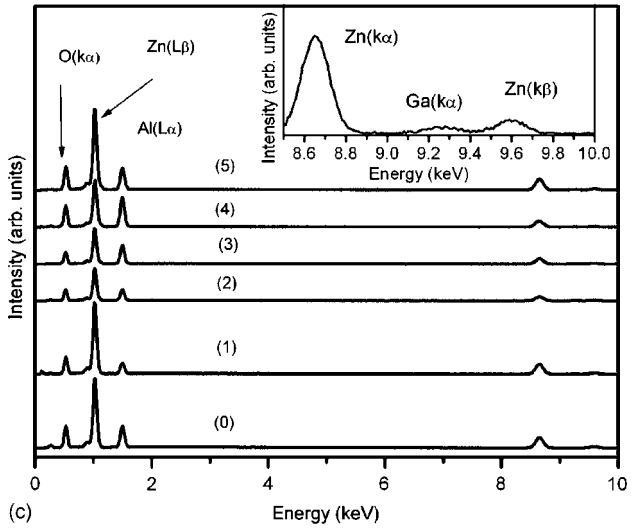

FIG. 2. (a) X-ray θ-2θ diffraction pattern from $Zn_{1-x}Ga_xO$ films with $x=0-0.05$. (b) X-ray Φ scan from $Zn_{1-x}Ga_xO$ film ($x=0.05$) for $(10\bar{1}1)$ plane. (c) EDS spectra from various $Zn_{1-x}Ga_xO$ films; inset is a close-up of $Zn_{0.95}Ga_{0.05}O$. Labels (0)–(5) correspond to at. % Ga concentration.

peaks at 60° intervals are consistent with the hexagonal symmetry of the epitaxial ZnO wurtzite structure.[15] Figure 2(c) shows the EDS spectra for $Zn_{1-x}Ga_xO$ films. Only six peaks

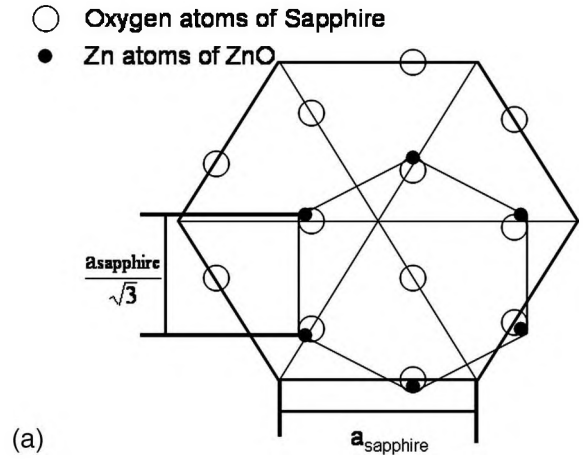

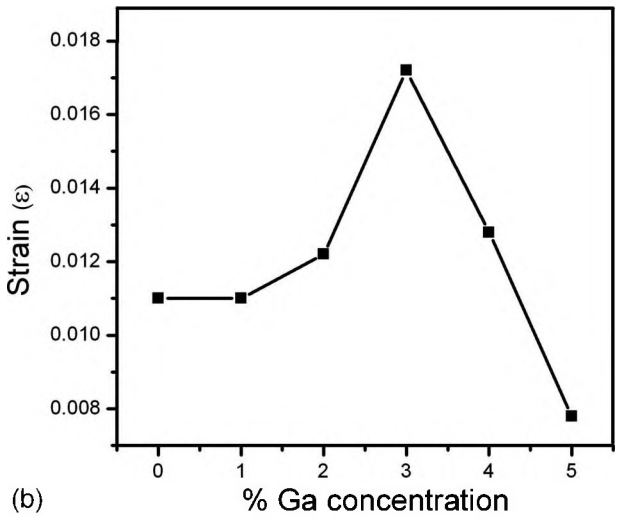

FIG. 3. (a) Schematic diagram illustrating the mechanism of epitaxial growth of $Zn_{1-x}Ga_xO$ on sapphire. Epitaxial growth occurs by domain matching epitaxy (DME) where six $(2\bar{1}\bar{1}0)$ planes of ZnO match with seven $(30\bar{3}0)$ planes of sapphire across the interface. (b) Variation in residual strain present in $Zn_{1-x}Ga_xO$ films as a function of Ga concentration.

corresponding to $Zn(L\beta)$,$(k\beta)$,$(k\alpha)$, $O(k\alpha)$, $Al(L\alpha)$, and $Ga(k\alpha)$ were observed indicating high phase purity. Quantitative elemental analysis showed that the stoichiometry of the films is very close to starting bulk materials.

Lattice parameters of ZnO are $a=3.252$ Å, $c=5.213$ Å and that of sapphire are $a=4.758$ Å, $c=12.991$ Å. So it is indeed quite interesting to see that even with such a huge lattice mismatch, $Zn_{1-x}Ga_xO$ grows epitaxially on sapphire (0001) substrate. Earlier studies have shown that the growth in this case occurs by a mechanism known as domain matching epitaxy (DME).[16] DME involves the matching of integral multiple (m) of lattice planes of the film with another integral multiple (n) of the lattice planes of the substrate. In the case of ZnO films on sapphire, six $(2\bar{1}\bar{1}0)$ planes of ZnO match with seven $(30\bar{3}0)$ planes of sapphire. Figure 3(a) shows a schematic diagram illustrating the domain matching mechanism in the case of $Zn_{1-x}Ga_xO$ on sapphire. In DME growth, residual strain in the film is given by the expression $\varepsilon_r = md_f/nd_{sub} - 1$, where d_f and d_{sub} are the interplanar spacings of planes matching at the interface. Figure 3(b) shows

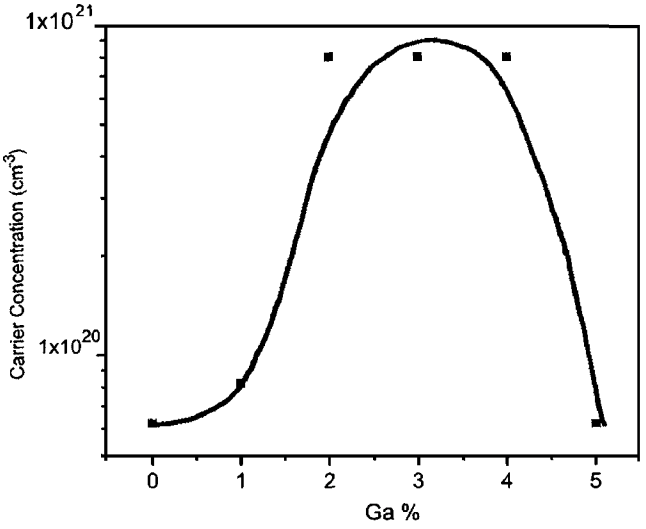

FIG. 4. Carrier concentration in $Zn_{1-x}Ga_xO$ x=0–0.05 films as determined by Hall effect measurement. The solid line is merely a guide for the eyes.

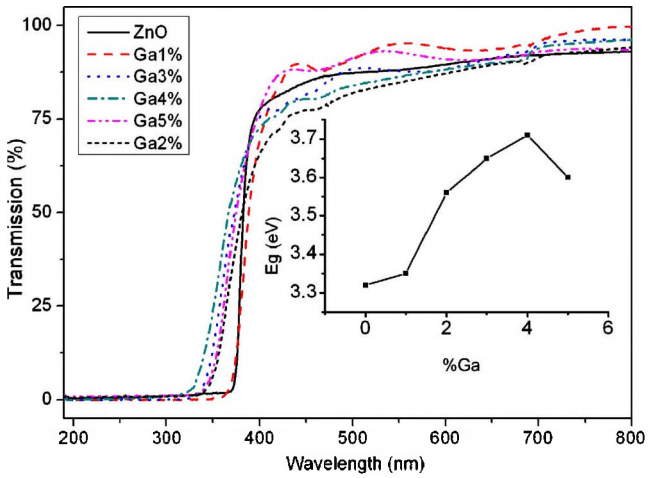

FIG. 5. Transmission spectra from $Zn_{1-x}Ga_xO$ (x=0–0.05) films. Inset shows the value of E_g as a function of Ga concentration.

the variation in residual strain values in $Zn_{1-x}Ga_xO$ films as Ga concentration x changes. Strain values were calculated for the matching of six $(2\bar{1}\bar{1}0)$ lattice planes of ZnO with seven $(30\bar{3}0)$ planes of sapphire. As can be seen in this figure, all $Zn_{1-x}Ga_xO$ films are under compressive stress with a maximum strain for x=0.03. The observed variation in the epitaxial strain of $Zn_{1-x}Ga_xO$ films with x arises because of the similar changes occurring in the lattice parameters of the bulk $Zn_{1-x}Ga_xO$ material [see Fig. 1(b)]. Specifically both the lattice parameters a and c of bulk $Zn_{1-x}Ga_xO$ show peaks at x=0.03, resulting in a maximum in the interplanar spacing of $(2\bar{1}\bar{1}0)$ planes. Since the interplanar spacing of $(30\bar{3}0)$ planes of sapphire remains unaffected by the variation in x, a peak in the interplanar spacing of $(2\bar{1}\bar{1}0)$ planes of $Zn_{1-x}Ga_xO$ results in a similar peak in the compressive strain.

Figure 4 shows carrier concentration in $Zn_{1-x}Ga_xO$ films as determined by Hall effect measurement at room temperature. For the undoped ZnO film, the carrier concentration was 6×10^{19} cm^3, which shows the presence of significant amount of oxygen vacancies in the system. As the Ga concentration is increased in the system, carrier concentration increases until 2% of Ga doping and then remains constant until 4%. On further increasing the Ga doping a decrease in carrier concentration is observed. The observed variation of carrier concentration with Ga doping is indeed very interesting; plausible mechanism responsible for this behavior is discussed later in this paper.

Figure 5 shows the transmission spectra from $Zn_{1-x}Ga_xO$ (x=0–0.05) films recorded over the wavelength range of 190–800 nm. As can be seen in the figure, all the films are very transparent with transmittance exceeding 90% over the whole visible range. The most important feature of the data is a systematic change in the absorption edge with increasing Ga concentration. As the Ga concentration increases, absorption edge moves towards the lower wavelengths until 4% Ga doping concentration. For 5% Ga doping the absorption band edge moves towards the higher wavelength side. By fitting the absorption edge to $\alpha\sim(h\nu-E_g)^{1/2}$, band gap values were estimated.[17] Inset of Fig. 5 shows the values of E_g as a function of Ga concentration. As can be seen in the figure, E_g increases with Ga concentration until a maximum is reached at 4% Ga and then a decrease is observed.

The observed variation of band gap and carrier concentration is expected to be the consequence of the combined effect of band filling (Burstein-Moss effect),[18,19] electronic correlation,[20,21] and the epitaxial strain,[22] present in the system. As the Ga is doped into ZnO, carrier concentration increases. However, since the undoped ZnO itself has quite high concentration of carriers, any further increase results in the filling of the bottom of conduction band. Figures 6(a) and 6(b) show filling of the conduction band as the carrier concentration exceeds the Mott critical density.[21] As the bottom of the conduction band is filled, more energy is needed to excite electrons from the donor impurity band to the conduction band, i.e., the ionization energy of Ga increases. Because of this increase, at high donor concentrations a continuous linear increase in carrier concentration with Ga doping level is not observed. Overall variation in carrier concentration is expected to be the consequence of the combined effect of increase in dopant concentration as well as in ion-

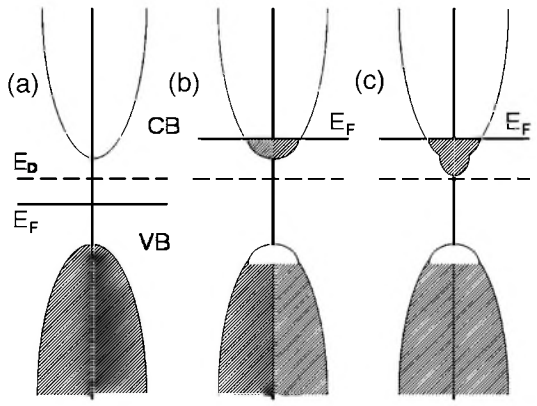

FIG. 6. Schematic diagram of the energy bands, (a) is at low impurity doping concentrations, (b) as concentration exceeds Mott's critical density, and (c) decrease in band gap due to band bending.

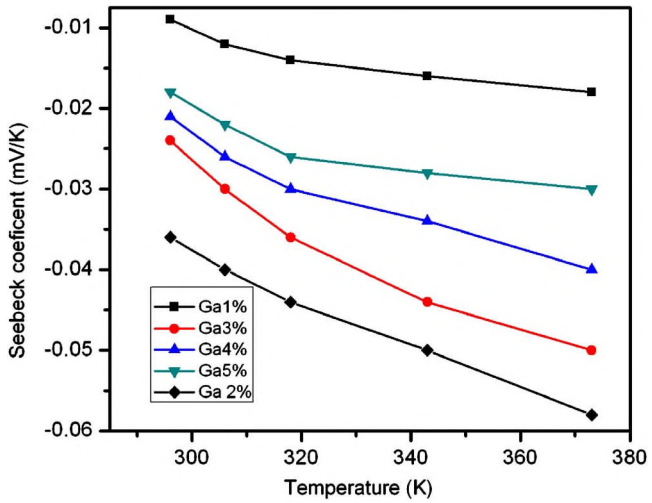

FIG. 7. Seebeck coefficient of $Zn_{1-x}Ga_xO$ (x=0–0.05) films over the temperature range of 296–373 K.

ization potential. Filling of the bottom of the conduction band is also responsible for the increase in the value of E_g for lower doping concentrations. For higher doping levels strong electron correlation effects may also become quite significant which can result in a decrease in the band gap.[20] Figure 6(c) shows a perturbed band structure which leads to a reduction in the band gap. At this point we want to mention that the epitaxial strain present in the films may also be playing quite an important role in the system.[22] As can qualitatively be seen in Fig. 3, epitaxial compressive strain shows quite similar variation with Ga concentration as carrier concentration and band gap. However, a slight difference in the peak positions in Fig. 3(b) (residual strain versus x), Fig. 4 (carrier concentration versus x), and Fig. 5 (E_g vs x) is observed. Here we find it in order to restate that the value of E_g depends on three competing factors: (i) carrier concentration, (ii) strain, and (iii) electronic correlation effects. Though we have experimentally determined the behavior of first two factors, a complete understanding about the third factor is still lacking. That could probably be the cause of the observed behavior.

Figure 7 shows the Seebeck coefficient of various $Zn_{1-x}Ga_xO$ (x=0–0.05) films measured over the temperature range 296–373 K. The thermoelectric power of all the samples is negative, which again confirms that electrons are the dominant charge carrier. Figure 8 illustrates variation of electrical resistivity of $Zn_{1-x}Ga_xO$ films at temperatures between 77 and 300 K. As can be seen in the figure, electrical resistivity depends very sensitively on the concentration of Ga in the films. Undoped ZnO films show a room temperature electrical resistivity of 0.036 Ω cm with a semiconductorlike temperature dependence. While in the films doped with 1% Ga a significant decrease in the electrical resistivity (1.44×10^{-4} Ω cm) is observed with a metal-like temperature dependence. Metallic behavior arises due to the large concentration of carriers (more than Mott's critical density[21]) introduced in the system. Because of the large carrier density, the electrons start filling the bottom of the conduction band and consequently the Fermi level resides in the conduction band resulting in the metallic behavior. On further increasing the Ga doping concentration, enhanced scattering potential resulting from randomly distributed impurity atoms causes Anderson localization of electronic states. As a result the material again starts showing a semiconductor-like negative temperature coefficient of resistivity. Quantitative analy-

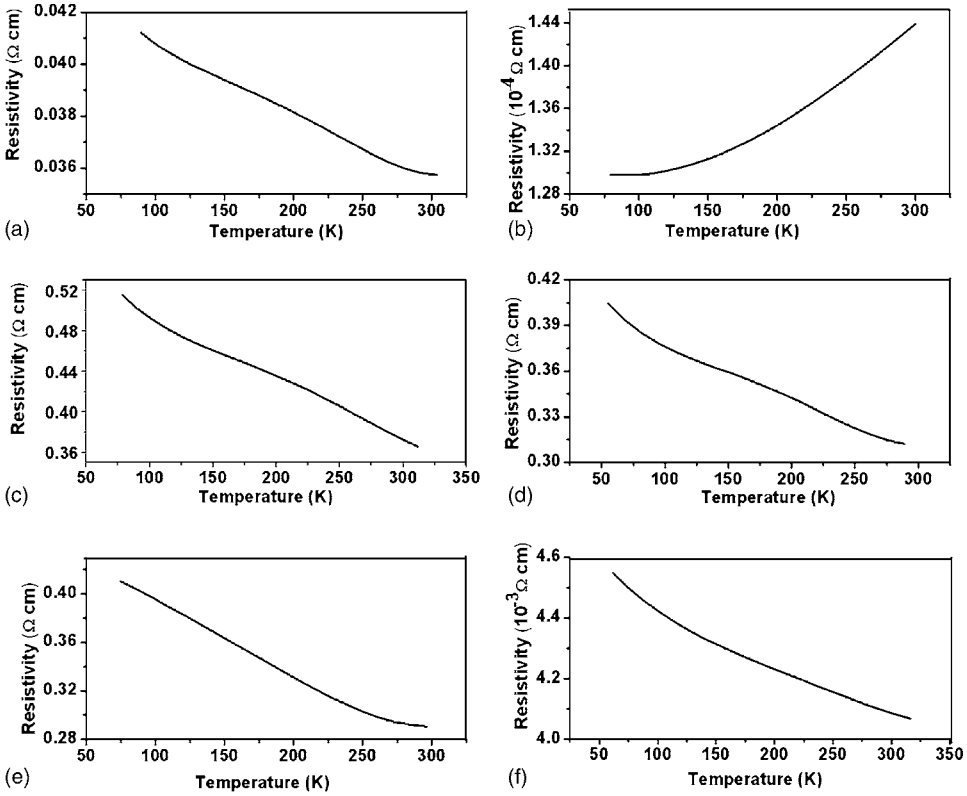

FIG. 8. Electrical resistivity of $Zn_{1-x}Ga_xO$: (a) x=0, (b) x=0.01, (c) x=0.02, (d) x=0.03, (e) x=0.04, and (f) x=0.05, films over the temperature range of 77–300 K.

sis of electrical resistivity data shows the variable range hopping (VRH) as the dominant conduction mechanism. Here we find it appropriate to mention that the electrical resistivity of $Zn_{1-x}Ga_xO$ thin films also depends on ambient oxygen pressure during the growth. In an earlier work Bhosle *et al.*[23] observed metal-insulator (*M-I*) transition for 1%–5% of Ga doping in $Zn_{1-x}Ga_xO$ films grown at 2×10^{-2} Torr of oxygen pressure. However, in the present study on $Zn_{1-x}Ga_xO$ films grown at the pressure of 10^{-6} Torr we could not observe any *M-I* transition.

CONCLUSION

In summary, we have grown epitaxial $Zn_{1-x}Ga_xO$ ($x=0-0.05$) films on single crystal *c*-plane sapphire substrates and investigated the structural, electrical, and optical properties as a function of Ga dopant concentration. Mechanisms responsible for the epitaxial growth of $Zn_{1-x}Ga_xO$ on highly lattice mismatched substrate were discussed. All the films were found to be under compressive stress. Epitaxial strain present in the films was estimated and was found to be a function of the Ga doping concentration. Carrier concentration and band gap in various $Zn_{1-x}Ga_xO$ films were determined using Hall effect and optical transmission measurements. Carrier concentration and optical band gap were found to first increase with increasing gallium concentration (until $x=0.04$) followed by a decrease at higher Ga concentration. These characteristics were found to be the consequence of the combined effect of band filling (Burstein-Moss effect), electronic correlation, and epitaxial strain present in the system. Electrical resistivity and thermoelectric power of the films were found to depend very sensitively on the concentration of Ga in the films. Undoped ZnO films showed a room temperature electrical resistivity of 0.036 Ω cm with a semiconductor-like temperature dependence. When 1% of Ga is doped in the material, a significant decrease in the electrical resistivity (1.44×10^{-4} Ω cm) was observed with a metal-like temperature dependence. Metallic behavior arises due to the large concentration of carriers (more than Mott's critical density) present in the system. Because of the large carrier density, the electrons fill the bottom of the conduction band. Consequently, the Fermi level resides in the conduction band resulting in metallic behavior. On further increasing the Ga doping concentration, enhanced scattering potential resulting from randomly distributed impurity atoms causes Anderson localization of electronic states.

ACKNOWLEDGMENTS

The authors want to thank Paul Slusser and David Toledo for help in some of the experiments. Financial support from the University of Utah Seed Grant program is thankfully acknowledged.

[1] B. G. Lewis and D. C. Paine, MRS Bull. **24**, 22 (2000).
[2] T. Minami, T. Miyata, and T. Yamamoto, J. Vac. Sci. Technol. A **17**, 1822 (1999).
[3] S. J. Pearton, D. P. Norton, K. Ip, Y. W. Heo, and T. Steiner, Prog. Mater. Sci. **50**, 293 (2005).
[4] U. Ozgur *et al.*, J. Appl. Phys. **98**, 041301 (2005).
[5] B. Thangaraju, Thin Solid Films **402**, 71 (2002).
[6] Y. Furubayashi, T. Hitosugi, Y. Yamamoto, K. Inaba, G. Kinodo, Y. Hirose, T. Shimada, and T. Hasegawa, Appl. Phys. Lett. **86**, 252101 (2005).
[7] A. Singh and R. Mehra, J. Appl. Phys. **90**, 5661 (2001).
[8] D. Zhang and D. Brodie, Thin Solid Films **213**, 109 (1992).
[9] V. Khranovskyy, U. Grossner, O. Nilsen, V. Lazorenko, G. Lashkarev, B. Svensson, and R. Yakimova, Thin Solid Films **515**, 472 (2006).
[10] S. M. Park, T. Ikegami, and K. Ebihara, Thin Solid Films **513**, 90 (2006).
[11] H. Ko, Y. Chen, S. Hong, H. Wenisch, and T. Yao, Appl. Phys. Lett. **77**, 3761 (2000).
[12] M. Snure and A. Tiwari, J. Nanosci. Nanotechnol. **7**, 481 (2007).
[13] M. Leszczynski *et al.*, Appl. Phys. Lett. **69**, 73 (1996).
[14] M. Leszczynski, J. Bak-Misiuk, J. Domagala, J. Muszalski, M. Kaniewska, and J. Marczewski, Appl. Phys. Lett. **67**, 539 (1995).
[15] I. Kim, Y. Kwon, J. Yi, J. Je, G. Nouet, T. Wojtowicz, P. Ruterana, and J. Kioseoglou, J. Vac. Sci. Technol. A **22**, 2159 (2004).
[16] J. Narayan and B. Larson, J. Appl. Phys. **93**, 278 (2003).
[17] A. Tiburcio-Silver, J. Joubert, and M. Labeau, J. Appl. Phys. **76**, 1992 (1994).
[18] E. Burstein, Phys. Rev. **93**, 632 (1954).
[19] T. Moss, Proc. Phys. Soc. London, Sect. B **67**, 775 (1954).
[20] B. Sernelius, K. Berggren, Z. Jin, I. Hamberg, and C. Granqvist, Phys. Rev. B **37**, 10244 (1988).
[21] N. F. Mott, *Metal-Insulator Transition* (Taylor & Francis, London, 1974).
[22] M. B. Ortuno-Lopez, M. Sotelo-Lerma, A. Mendoza-Galvan, and R. Ramirez-Bon, Vacuum **76**, 181 (2004).
[23] V. Bhosle, A. Tiwari, and J. Narayan, J. Appl. Phys. **100**, 033713 (2006).